



HHS Public Access

Author manuscript

Nat Neurosci. Author manuscript; available in PMC 2014 September 01.

Published in final edited form as:

Nat Neurosci. 2014 March ; 17(3): 423–430. doi:10.1038/nn.3632.

Basal Ganglia Subcircuits Distinctively Encode the Parsing and Concatenation of Action Sequences

Xin Jin^{1,3,*}, Fatuel Tecuapetla², and Rui M Costa^{1,2,*}

¹Laboratory for Integrative Neuroscience, National Institute on Alcohol Abuse and Alcoholism, National Institutes of Health, 5625 Fishers Lane, Bethesda, Maryland 20892, USA

²Champalimaud Neuroscience Programme at Instituto Gulbenkian de Ciência and Champalimaud Center for the Unknown, Av. de Brasília, Lisbon 1400-038, Portugal

³Molecular Neurobiology Laboratory, Salk Institute for Biological Studies, 10010 North Torrey Pines Road, La Jolla, California 92037, USA

Abstract

Chunking allows the brain to efficiently organize memories and actions. Although basal ganglia circuits have been implicated in action chunking, little is known about how individual elements are concatenated into a behavioral sequence at the neural level. Using a task where mice learn rapid action sequences, we uncovered neuronal activity encoding entire sequences as single actions in basal ganglia circuits. Besides start/stop activity signaling sequence parsing, we found neurons displaying inhibited or sustained activity throughout the execution of an entire sequence. This sustained activity covaried with the rate of execution of individual sequence elements, consistent with motor concatenation. Direct and indirect pathways of basal ganglia were concomitantly active during sequence initiation, but behaved differently during sequence performance, revealing a more complex functional organization of these circuits than previously postulated. These results have important implications for understanding the functional organization of basal ganglia during the learning and execution of action sequences.

Memory, perception and action often require dealing with more or less complex series of elements^{1–3}. It has been proposed that the brain can organize individual elements of memories or action sequences into a single unit, allowing for more reliable recall or efficient performance^{1–3}. This process is especially relevant for action sequences that need extremely fast and precise control, notably human speech and animal vocalization⁴. Organizing such actions is slow and progressive, and requires efficient concatenation of elemental actions into one behavioral unit^{1,2,5}. Basal ganglia circuits have been proposed to be involved in organizing motor and cognitive actions into chunks^{6,7}. Indeed, dysfunction of basal ganglia

Users may view, print, copy, and download text and data-mine the content in such documents, for the purposes of academic research, subject always to the full Conditions of use:http://www.nature.com/authors/editorial_policies/license.html#terms

*To whom correspondence should be addressed. rui.costa@neuro.fchampalimaud.org (R.M.C.) or xjin@salk.edu (X.J.).

AUTHOR CONTRIBUTIONS

X.J. performed the experiments and analyzed the data. F.T. conducted part of the D2-Cre optogenetics experiment. X.J. and R.M.C. designed the experiments and wrote the manuscript.

The authors declare no conflicts of interest.

in both animals^{8–10} and humans^{11–13} has been associated with deficits in action sequence organization and chunking. Consistently, previous studies have shown that neuronal activity related to the initiation and termination of action sequences emerges in nigrostriatal circuits during sequence learning^{9,14}. Furthermore, it has been recently shown that the BOLD signal in sensorimotor striatum is correlated with the concatenation of motor sequences¹⁵. However, there is little understanding of how individual elements are concatenated into unitary action sequences, as well as how behaviorally discrete sequences are identified and separated in basal ganglia circuits. We developed a novel behavioral paradigm to study the activity of basal ganglia circuits while mice learn to perform extremely rapid action sequences, on the temporal scale of human speech¹⁶, and uncovered that neural activity related to the execution of whole action sequences rather than unitary elements emerges in basal ganglia circuits during sequence learning.

Basal ganglia circuits encompass two major pathways: a monosynaptic GABAergic projection from dopamine D1 receptors-expressing striatal medium spiny projection neurons (striatonigral MSNs) to the output nuclei like substantia nigra pars reticulata (SNr), called ‘direct pathway’^{17,18}; and a polysynaptic projection from dopamine D2 receptors-expressing striatal medium spiny projection neurons (striatopallidal MSNs) to output nuclei through external globus pallidus (GPe) and subthalamic nucleus (STN), named ‘indirect pathway’^{17,18}. Classical models of basal ganglia circuit function suggest that the direct and indirect pathway are differentially modulated by dopamine, and work in an antagonistic manner to facilitate or inhibit movement, respectively^{19–22}. However, other models propose that the coordinated activity of both direct and indirect pathways is critical for actions^{23,24}. We therefore used multisite recordings and optogenetics to investigate how activity related to the parsing and concatenation of action sequences developed in basal ganglia circuits, and if these activities were distinctly implemented in the direct and indirect basal ganglia pathways.

RESULTS

Mice learn to perform rapid action sequences

We trained mice to perform gradually faster sequences of lever presses until they reached the limit of their performance. Mice ($n = 29$) were first trained in a self-paced operant task where four consecutive lever presses lead to a sucrose reward (fixed-ratio four, FR4)⁹. After six days of FR4 training, mice were then advanced into a differential reinforcement schedule where four consecutive lever presses performed within a particular time window (FR4/Xs, fixed-ratio four within X seconds) would lead reward (see Methods). The duration of time required to perform the four lever presses was reduced across sessions from 8s, to 4s, to 2s, to 1s and finally to 0.5s (from 0.5 Hz to 8Hz). Mice learned to perform the sequences of lever presses faster as training progressed, as evidenced by both the gradual decrease in the average inter-press interval (IPI) and the clustering of consecutive IPIs closer to the final target sequence (Fig. 1a, 13.3%, 15.0%, 30.7%, 42.4%, and 48.0% of consecutive IPIs occurring below the 500 ms quadrant for the five training schedules respectively). In the final stage of training, as animals performed under the 8Hz schedule, the peak distribution of IPIs fell below 167ms which is the average IPI duration required for rewarded sequences

under FR4/0.5s schedule (Fig. 1b). We quantified each IPI within a rewarded sequence⁹ (Fig. 1c), and found that the first, second and third within-sequence IPIs all decreased consistently throughout learning (Fig. 1d, two-way ANOVA test, main effect of training $F_{4, 264} = 199.80$, $P = 1.4 \times 10^{-78}$; main effect of IPI $F_{2, 66} = 10.01$, $P = 0.0002$; no interaction between training and IPI $F_{4, 64} = 1.71$, $P = 0.10$). The variability of first, second and third IPI, measured as coefficient of variance⁹, also significantly decreased during training (Fig. 1e, two-way ANOVA test, $F_{4, 264} = 33.03$, $P = 2.5 \times 10^{-22}$), showing that each animal performed more similar sequences of presses as training progressed. This means that the decrease in variability did not simply result from progressively increasing response rate, but that the standard deviation of the IPIs decreased disproportionately faster than the mean of the IPIs (Supplementary Fig. 1). At the end of training, the range of variability of these ultrafast sequences after training was comparable to other learned or innate action sequences reported in different species^{9,25,26}. As the degree of difficulty of the task increased, action efficiency, measured by the percentage of rewarded lever presses out of total lever presses, decreased through faster schedules (from ~80% under FR4/8s to ~7% under FR4/0.5s, one-way ANOVA test, $F_{4, 140} = 94.46$, $P = 9.0 \times 10^{-39}$). However, sequence length increased to average 4 presses per sequence after 6 days of FR4 training⁹ (shorter than four on day 1, unpaired t-test, $t_{28} = 7.40$, $P = 0.0001$ and no difference to four on day 6, $t_{28} = 0.27$, $P = 0.79$), although during this phase of training animals would get a reward every 4 presses whether those 4 presses occurred consecutively in a sequence or not (e.g. 2 sequences of 2 presses would earn one reward, and one sequence of 8 presses would earn 2 rewards). What is more, the mice continued to consistently press about 4 times per sequence across different fast sequence schedules (Fig. 1f, different from four, unpaired t-test, $t_{28} = 3.29$, $P = 0.003$ for 0.5Hz, $t_{28} = 0.98$, $P = 0.34$ for 1Hz, $t_{28} = 1.33$, $P = 0.20$ for 2Hz, $t_{28} = 1.15$, $P = 0.26$ for 4Hz and $t_{28} = 0.64$, $P = 0.53$ for 8Hz), showing that they learned to perform sequences of 4 presses within a certain time limit, and with little within-animal variability in inter-press intervals. Importantly, the proportion of successful ultrafast sequences (sequences of 4 presses in 0.5s, close to the limit of every animal we trained) significantly increased with training (from virtually none early in training, Fig. 1g, one-way ANOVA test, $F_{4, 140} = 3.42$, $P = 0.01$). Taken together, these data indicate that mice were able to learn and chunk rapid action sequences (Supplementary Movie 1),

As it was previously shown that striatal plasticity was important for sequence learning⁹, we next tested if striatal plasticity was necessary for the appropriate balance between speed and accuracy in the execution of these rapid sequences. We crossed mice expressing Cre recombinase in medium spiny neurons (RGS9L-cre), with mice carrying a floxed allele of the NMDAR1 gene. Although the resulting *RGS9L-Cre/Nr1^{fl/fl}* mice could learn to press rapidly, they had more variable sequences, with the average number of lever presses more distant to the target number (four) than control littermates. This suggests that striatal plasticity was not necessary for rapid motor performance but rather for the appropriate organization of these homogeneous sequences of 4 elements. Consistently, this resulted in lower action efficiency in mutants than controls despite the higher within-sequence press rate (Supplementary Fig. 2), confirming that striatal plasticity is required for organization of the number of elements in action sequences⁹.

Striatum encodes entire sequences as single actions

We implanted electrode arrays (see Methods) in the dorsal striatum and its downstream projection nuclei substantia nigra pars reticulata (SNr) and external globus pallidus (GPe) (Supplementary Fig. 3, Supplementary Table 1), and recorded neuronal activity while mice learned rapid action sequences. We analyzed the microstructure of each lever press sequence, and the neuronal activity related to each lever press within an action sequence⁹. Peri-event histograms (PETHs) were calculated based on the alignment to the first, second, third, fourth or final press (some sequences had more than four presses) for all rewarded action sequences (Fig. 2a). Consistent with previous studies⁹, we found MSNs with activity related to the initiation or termination of a sequence of presses (start/stop activity) (Fig. 2a, b; Supplementary Fig. 4, Supplementary Fig. 5, Supplementary Table 1), which can signal the parsing of presses into sequences. However, we uncovered that many MSNs displayed changes in activity related to the execution of the entire sequence of presses. Many MSNs decreased firing rate throughout the whole lever-press sequence (inhibited, Fig. 2c, Supplementary Fig. 5), while others displayed an increase in activity throughout the whole sequence (sustained, Fig. 2d, Supplementary Fig. 5). There were almost no cells showing selective firing only to the second or third lever press ($< 5\%$)⁹. What is more, this sequence-related sustained activity oscillated with a frequency related to the lever press-frequency in each sequence (Pearson's $R = 0.55$, $P = 7.8 \times 10^{-79}$, Fig. 2h), and in total almost 95% of MSNs with sustained activity exhibit this type of significant correlation (Fig. 2i). Importantly, this correlation was absent for neurons displaying either start/stop or inhibited sequence-related activity. The percentage of MSNs showing sequence-related start/stop activity (Fig. 2e, one-way ANOVA test, no effect of training $F_{4, 48} = 0.21$, $P = 0.93$) and sequence-related inhibited activity (Fig. 2f, one-way ANOVA test, no effect of training $F_{4, 48} = 0.35$, $P = 0.84$) remained relatively stable while animals progressed from 0.5 Hz to 8Hz. However, the percentage of MSNs showing sequence-related sustained activity (Fig. 2g, one-way ANOVA test, main effect of training $F_{4, 48} = 3.91$, $P = 0.008$, for more details see Supplementary Fig. 6, Supplementary Fig. 7) decreased slightly through training, suggesting a process of refinement and selection of these neural correlates of motor concatenation as training progressed. These results show that during action sequence learning, neural activity signaling whole action sequences as one action unit appears in striatum.

GPe and SNr exhibit different sequence-related activity

The finding that the proportion of MSNs with sequence-related activity did not change much as the training schedules progressed could stem from the fact that in these analyses different MSN types which project to different targets (striatonigral and striatopallidal), were grouped together. We therefore investigated the evolution of sequence-related activity in the target nuclei SNr and GPe, which receive GABAergic afferents from the striatum to form the direct and indirect pathways^{17,18}. We found all three types of sequence-related activity in these two nuclei (start/stop, inhibited and sustained, Fig. 3a–c; Pearson's $R = 0.50$, $P = 2.3 \times 10^{-45}$ in Fig. 3g; Supplementary Table 1). However, we found that the proportion of neurons showing these different types of sequence-related activity evolved differently in SNr and GPe as training progressed (Fig. 3d–f). With training more neurons displayed sequence-

related start/stop activity in SNr than GPe (Fig. 3d, two-way ANOVA test, main effect of region $F_{1, 17} = 14.04$, $P = 0.0004$). Similarly, a higher proportion of neurons displayed sequence-related inhibited activity in SNr than GPe as training progressed (Fig. 3e, two-way ANOVA test, main effect of region $F_{1, 17} = 38.90$, $P = 9.0 \times 10^{-6}$; interaction between training and region $F_{4, 14} = 4.33$, $P = 0.004$). In contrast, more neurons exhibiting sequence-related sustained activity emerged in GPe than SNr (Fig. 3f, two-way ANOVA test, main effect of region $F_{1, 17} = 10.40$, $P = 0.002$; interaction between training and region $F_{4, 14} = 2.29$, $P = 0.07$, for more details see Supplementary Fig. 6, Supplementary Fig. 7). Interestingly, the sustained activity of SNr neurons was on average less related to lever press-frequency than that of GPe neurons (Fig. 3h, i, chi-square test, $\chi^2 = 15.79$, $P = 0.0004$). Taken together, these data suggest that direct versus indirect basal ganglia pathways are differentially involved in action sequence learning and performance.

Sequence activity is action-specific but speed-generalized

Sequence-related activity in basal ganglia circuits may simply result from the rapid performance of different motor elements close in time or really encode specific action sequences. To disambiguate between these possibilities, we trained a subgroup of mice ($n = 9$) to perform two sessions in the same day, either under the same schedule/speed requirement but on different action sequences (left vs. right lever) or under different schedules/speeds (e.g. 4Hz vs. 8Hz) on the same action sequence⁹ (Methods). This experiment permitted us to track the same neuron's activity during the performance of different action sequences at the same speed, or the same action sequence at different speeds. We found that the majority of neurons with start/stop activity in the striatum, SNr and GPe were action-specific (Fig. 4a–c). Sustained and inhibited activity in these regions also showed some action-specificity, with the exception of neurons in DS with inhibited activity, which showed similar sequence-related inhibited activity for different actions (paired t-test, $t_4 = 1.00$, $P = 0.37$), suggesting that they may have a more permissive role in action execution. In contrast, very few neurons with sequence-related activity were speed-specific (Fig. 4a–c), indicating that the majority of neurons in these circuits exhibited similar start/stop, inhibited and sustained activity across different speeds of sequence performance (two-way ANOVA test, no effect of activity type $F_{2, 86} = 2.82$, $P = 0.06$; no effect of region $F_{2, 43} = 0.43$, $P = 0.65$; no interaction between activity type and region $F_{4, 41} = 0.72$, $P = 0.58$). These data suggested that the sequence-related activity uncovered here reflects the chunking of particular actions and not so much the rapid performance of different motor elements close in time^{9,23,24,27}

D1- and D2-MSNs distinctively encode parsing and concatenation

The results above suggest that basal ganglia circuits differentially encode action sequences, and hence that striatonigral and striatopallidal MSNs, which project to SNr and GPe respectively^{17,18}, should behave differently during rapid sequence performance. We thus sought to investigate if these subtypes of MSNs (D1- versus D2-expressing) displayed different sequence-related activity by using photostimulation-assisted cell identification^{9,28}. We expressed light-activated channel channelrhodopsin-2 (ChR2)²⁹ in D1 versus D2-MSNs by injecting AAV viruses expressing ChR2 in a Cre-dependent manner into the striatum of mice expressing Cre recombinase specifically in these neurons¹⁸ (Fig. 5a, b). A customized

electrode array attached with a guide cannula, which terminates at 300 μ m above the electrode tips (Fig. 5c, Methods), was implanted into the same location of dorsal striatum. This specific design allowed us to insert the optic fiber through the cannula, and more importantly, to carefully adjust its position to reach optimal light stimulation for identification of different cells in each session. We trained this new group of mice to perform the task; after training was completed recordings were performed in normal sessions followed by light stimulation in the end of each session. A series of rather strict criteria to considering direct activation by light were used for cell identification. Only those units activated by light delivery, with short-latency (≤ 6 ms) to light response, and displaying identical waveforms during the behavioral session and light stimulation (Pearson's $R = 0.95$) were considered to be direct or indirect pathway MSNs^{9,28} (Fig. 5e, g, i, j; mean latency for positively identified D1-MSNs 3.8 ± 0.1 ms, mean latency for positively identified D2-MSNs 3.9 ± 0.1 ms, unpaired t-test, no significant difference $t_{261} = 1.09$, $P = 0.28$; Supplementary Table 1, also see Methods). The latency of ChR2-evoked responses in vivo for D1-/D2-MSNs has been reported as much as 40 ms or longer²². Although much stricter criteria were utilized in this study to minimize the possibility of false positives, the results and the conclusions were qualitatively consistent if more loose criteria were used (for example with longer response latency ≤ 10 ms, Supplementary Fig. 8).

Analyses of the results from five D1-ChR2 mice ($n = 121$ positively identified cells in total from multiple sessions; Supplementary Table 1) and five D2-ChR2 mice ($n = 142$ positively identified cells in total from multiple sessions; Supplementary Table 1) showed that although a slightly higher proportion of D1-MSNs displayed start/stop activity than D2-MSNs, this difference was not significant (Fig. 5d, e, k, unpaired t-test, $t_{19} = 0.80$, $P = 0.44$). In contrast, sequence-related inhibited activity (Fig. 5f, g) was more predominant in D2-MSNs than in D1-MSNs (Fig. 5k, unpaired t-test, $t_{19} = 4.55$, $P = 2.2 \times 10^{-4}$), while the sequence-related sustained activity (Fig. 5h, i) was preferentially observed in D1-MSNs and less in D2-MSNs (Fig. 5k, unpaired t-test, $t_{19} = 2.37$, $P = 0.03$). This profile mirrored the distribution of sequence-related activity in downstream nuclei SNr and GPe, where SNr exhibited more sequence-related start/stop (Fig. 5l, unpaired t-test, $t_{10} = 2.89$, $P = 0.02$) and inhibited (Fig. 5l, unpaired t-test, $t_{10} = 3.14$, $P = 0.01$) activity than GPe, which had more sequence-related sustained (Fig. 5l, unpaired t-test, $t_{10} = 2.53$, $P = 0.03$) activity; and it is consistent with the fact that these two nuclei receive GABAergic inhibitory inputs from D1- and D2-MSNs respectively^{17,18}. These data indicate that direct and indirect pathways show concomitant activity during the initiation of action sequences, but behave rather differently during the execution of action sequences.

Surprisingly, when we further subdivided the start/stop activity in D1-/D2-MSNs into start only, stop only, and boundary (both start and stop) subtypes, we found that a similar percentage of D1-MSNs signaled sequence start vs. stop (Fig. 5m, paired t-test, $t_{11} = 0.47$, $P = 0.65$; Supplementary Fig. 8), while the majority of D2-MSNs preferentially displayed activity related to the start rather than the end of the sequence (Fig. 5m, paired t-test, $t_8 = 2.46$, $P = 0.04$; Supplementary Fig. 8). There was no significant difference in terms of timing of start activity between D1- and D2-MSNs populations (although D2-MSNs tended

to start slightly earlier, Supplementary Fig. 8). As in previous studies⁹, few D1 and D2-MSNs displayed boundary type activity compared to start only and stop only activity (Fig. 5m, paired t-test, $t_{11} = 6.71$, $P = 3.4 \times 10^{-5}$, and equal proportion in D1 vs. D2-MSNs, unpaired t-test, $t_{19} = 0.31$, $P = 0.76$). Notably, different types of putative striatal interneurons also showed distinct sequence-related activity (Supplementary Fig. 9). Furthermore, previous studies using a cue-instructed action sequence task have revealed that many neurons in cortex represent sequence boundaries³⁰. Consistently, when we investigated the activity of primary motor cortex (M1) neurons during sequence performance, we found that about half the neurons displayed start/stop activity, and that many M1 neurons encoded the sequence boundary (Supplementary Fig. 10), i.e., the same neuron changing rate during both sequence start and stop. Notably, few M1 neurons showed sustained activity throughout the whole sequence execution (Supplementary Fig. 10).

DISCUSSION

The results presented here show that when mice learn to perform very rapid action sequences as individual behavioral units, neuronal activity that encodes the whole sequence as one single action emerges in basal ganglia circuits. Besides activity related to the initiation and termination of the whole sequence, which could signal the parsing of single elements into sequences, we found neurons that changed their firing rate during the whole period of sequence execution. A subset of these neurons displayed sustained activity throughout the execution of the entire action sequence, and showed oscillations in firing rate that were correlated with the pressing rate. Others were inhibited throughout the whole duration of the sequence. These findings thus revealed that neurons in the basal ganglia might be involved in the concatenation of individual behavioral elements into motor chunks. Furthermore, optogenetic identification of cell types in behaving animals showed that striatonigral and striatopallidal neurons (D1 vs. D2-MSNs) show preferentially sequence-related sustained versus inhibited activity, respectively. Importantly, the target regions which receive GABAergic innervation from striatonigral and striatopallidal neurons (SNr and GPe) behave in a symmetric way, confirming that the two basal ganglia pathways have different activity during the execution of motor sequences (Supplementary Fig. 10).

This behavior of basal ganglia pathways during the performance of action sequences is consistent with well-accepted models of basal ganglia function postulating that direct pathway neurons would be active during movement to facilitate it, i.e. prokinetic; while indirect pathway neurons would be inhibited during movement and active during lack of movement, and hence be antikinetic^{19–22}. However, our optogenetic identification results clearly show that direct and indirect pathway neurons exhibiting a concomitant phasic increase in activity during the initiation of action sequences (Fig. 5m; Supplementary Fig. 8). These results are more consistent with alternative models that defend that co-activation of direct and indirect pathways is critical for action selection during movement initiation^{23,24}. Some, for example, defend that co-activation of these pathways would permit direct pathway neurons to select the desired motor program while indirect pathway neurons inhibit competing motor programs^{23,24}. Interestingly, D2-MSNs did tend to show slightly earlier phasic activity than D1-MSNs during sequence initiation, although these differences were not significant (Supplementary Fig. 8). Importantly, most of the start/stop activity that

we observed in basal ganglia circuits was specific to either the initiation or the termination of lever press sequences, suggesting that the basal ganglia deal with the specific movements starting and ending a motor sequence⁹, and not so much with defining the boundaries of the sequence (previously observed in striatum in maze tasks^{14,31}), which appears to be a more prominent feature of cortical areas (Supplementary Fig. 10)^{6,7,30,32,33}. These data thus strongly suggest that there may be different functional modes of basal ganglia during the initiation vs. execution of actions, which involve different subsets of D1-/D2-MSMs^{23,24} (Supplementary Fig. 10). Furthermore, this diversity in activity during sequence initiation versus sequence execution was observed also in the downstream target nuclei. For example, different subsets of neurons in SNr, which is thought to facilitate movement via disinhibition of target structures, displayed different sequence-related activity (start/stop, inhibited and even sustained). One interesting possibility would be that different subsets of SNr neurons project to different target areas^{34,35} and coordinate the activity in those areas during action sequences.

We observed virtually no neurons in basal ganglia with activity specifically related to the 2nd press or to the 3rd press of a sequence, suggesting that basal ganglia neurons can encode concatenation of motor elements at the individual neuron level. This is different from cerebral cortex, where sequential activation of different neurons at different time points³⁶ or selective activation of a specific neuron depending on the particular aspect of temporal structure of sequence^{33,37} have been observed. Still, the sustained activity observed in basal ganglia may result from the convergence of different upstream neurons into single striatal neurons; or from re-entrant cortico-basal ganglia-thalamus loops^{23,33,34,35}.

In summary, these findings indicate that the basal ganglia may be important not only for action selection but also for the modulation of ongoing actions^{38,39}. Also they reveal that different subsets of direct and indirect pathway neurons are engaged during sequence initiation, execution and termination, and suggest that the behavior of basal ganglia circuits during complex behavior may not obey to simple dichotomies. The data in the present study underscore the importance of basal ganglia circuits in the concatenation and parsing of action sequences, and thus their fundamental role in learning and organization of behavior. These findings may have important implications for understanding the neurological and psychiatric disorders where action chunking is affected, including Parkinson's and Huntington's diseases^{11,12}, obsessive-compulsive behavior⁴⁰, and speech disorders⁴¹.

METHODS

Animals

All experiments were approved by the NIAAA ACUC and the Portuguese DGV, and done in accordance with NIH and European guidelines. C57BL/6J male mice between 3 and 6 months old, purchased from the Jackson Laboratory at 8 weeks of age, were used in the WT experiments. Striatal-specific NMDAR1-knockout (KO) and control littermates were generated by crossing *RGS9-cre* mouse with *NMDAR1-loxP* mouse, as formerly described^{9,42}. *RGS9L-Cre/Nr1f/f* mice were backcrossed into C57Bl/6J. 2 to 6 months old male and female *RGS9L-Cre/Nr1f/f* homozygous mice and their littermate controls were used for behavioral experiments. BAC transgenic mice that express Cre recombinase under

the control of dopamine D1 receptor (EY217) or D2 receptor promoter (ER43) obtained from GENSAT¹⁸ were used for behavior, channelrhodopsin-2 (ChR2) expression and recording at 2 to 4 months of age. In the striatum, the D1 Cre and D2 Cre expression were mostly restricted to medium-spiny projection neurons but very little if any in interneurons^{18,22}. Mice were maintained in individually ventilated cages under a 12 hour light/dark cycle, and were group housed for the behavioral experiments and single housed for electrophysiology. RGS9L-Cre/Nr1f/f mice and control littermates (Cre-) were trained as cohorts at the same time. Experimenters were blind to the genotype in the experiments using RGS9L-Cre/Nr1f/f mice.

Behavioral training

Behavioral training took place in exactly same operant chambers described previously⁹. Briefly, each chamber (21.6 cm L × 17.8 cm W × 12.7 cm H) was housed within a sound attenuating box (Med-Associates, St. Albans, VT) and equipped with two retractable levers on either side of the food magazine and a house light (3 W, 24 V) mounted on the opposite side of the chamber. Sucrose solution (10%) through a syringe pump or food pellets (20mg) through a dispenser were delivered into the magazine as reinforcers. Magazine entries were recorded using an infrared beam and licks using a contact lickometer. Mice were placed on food restriction throughout training, and fed daily after the training sessions with ~2.5 g of regular chow so they would maintain around 85% of normal body weight.

Animals were first trained to acquire a regular sequence task under fixed-ratio 4 schedule as described before⁹. Training started with a 30 minute magazine training session in which the reinforcer was delivered on a random time schedule, on average every 60 seconds (30 reinforcers). The following day lever-pressing training started with continuous reinforcement (CRF), in which animals obtained a reinforcer after each lever press. After three days of CRF, regular sequence training of fixed-ratio four (FR4) started in which every four times of lever presses earn a reinforcer, and this training continued for six days. In the following day, rapid sequence training started where a differential reinforcement schedule was introduced. Reward was now delivered only when four times of lever presses finished within a particular time window, starting from 8s (FR4/8s) and gradually decreased day by day to 4s (FR4/4s), 2s (FR4/2s), 1s (FR4/1s) and finally to 0.5s (FR4/0.5s). A shorter time window was introduced when the animal could earn more than 20 reinforcers within a session of two hours. Throughout all training schedules, there was no explicit stimulus signaling when four presses were completed or when the reinforcer was delivered⁹. The animals were trained daily without interruption and every day the training started at approximately same time in the morning. The whole training process to reach rapid sequence performance of FR4/0.5s takes 3–4 weeks, and most (>85%) C57BL/6J mice can achieve FR4/1s or faster (FR4/0.5s) if trained properly. All timestamps of lever presses, magazine entries and licks for each animal were recorded with a resolution of 10 ms. The training chambers and procedures for RGS9L-Cre/Nr1f/f and littermate controls, as well as D1-ChR2 and D2-ChR2 mice were the same as used for C57BL/6J mice.

Sequence quantification

The beginning and end of a sequence of lever presses was determined by either the statistics of lever pressing for each animal (either bimodal or Poisson distribution, on average a 1s pause between sequences, also see Fig. 1b, c), or by a bout of licks interrupting lever pressing after reward delivery⁹. The sequence length and duration were thus calculated based on each individual sequence, and the within-sequence press rate computed by the ratio of sequence length (3 presses) and the corresponding sequence duration. The mean within-sequence inter-press interval (IPI) was calculated from inter-press intervals within each individual sequence, and averaged for all sequences in each animal for each session⁹. Action efficiency was defined as the percentage of rewarded lever presses out of total lever presses within a session under a particular schedule. The coefficient of variance (CV) was used to quantify the variability of inter-press intervals across learning, and it was mathematically defined as the ratio between the standard deviation and the mean of IPI.

Surgery and implantation

Electrophysiological data from C57BL/6J recording experiments on rapid sequence learning were collected from twenty one mice, and data in D1-/D2-ChR2 recording experiment on D1-/D2-MSNs identification were collected from additional ten mice (for details see Supplementary Table 1). Mice were implanted with one or two electrode arrays⁹, in the latter case either ipsilaterally with one targeting for the dorsal striatum (DS) and another for the substantia nigra pars reticulata (SNr), or bilaterally for DS and external global pallidus (GPe) or primary motor cortex (M1). For DS, 2 × 8 array of Platinum-coated tungsten microwire electrodes (Innovative Neurophysiology, Durham, NC) of 50 μm diameter with 150 μm spacing between microwires, and 250 μm spacing between rows were used. For SNr or M1, 2 × 8 Platinum-coated tungsten microwire electrodes of 35 μm diameter with 150 μm spacing between electrodes and 200 μm spacing between rows were used. For GPe, 4 × 4 Platinum-coated tungsten microwire electrodes of 35 μm diameter with 200 μm spacing between electrodes and 200 μm spacing between rows were used. In some experiments the array used for SNr was cut at a ~30 degree angle to better fit the medial-lateral anatomy of the SNr (Supplementary Fig. 3).

The craniotomies were made at the following coordinates: for ipsilateral DS and SNr, 0.5 mm rostral to bregma and 1.8 mm laterally for DS, 3.4 mm caudal to bregma and 1.0 mm laterally for SNr; for bilateral DS and GPe or M1, 0.5 mm rostral to bregma and 2.0 mm laterally for DS, 0.5 mm caudal to bregma and 1.8 mm laterally for GPe, 0.5 mm rostral to bregma and 1.1 mm laterally for M1. During surgeries, the microwire arrays were gently lowered ~ 2.2 mm from the surface of the brain for DS, ~ 4.4 mm for SNr, ~ 3.5 mm for GPe and ~ 1.0 – 1.1 mm for M1. The final placement of electrodes was monitored online during the surgery based on the neural activity, and confirmed histologically in the end of experiments after perfusion with 10% formalin, brain fixation in a solution of 30% sucrose and 10% formalin, followed by cryostat sectioning (coronal slices of 40 – 60 μm) and cresyl violet staining (Supplementary Fig. 3 and Supplementary Fig. 7).

For viral expression of channelrhodopsin-2 (ChR2) in D1-/D2-Cre mice, a cre-inducible adeno-associated virus (AAV) vector carrying the gene encoding the light-activated cation

channel channelrhodopsin-2 and a yellow fluorescent reporter (DIO-ChR2-YFP)^{9,22,28,29} was stereotactically delivered into the DS of D1-Cre or D2-Cre mice enabling specific expression of ChR2 in striatal D1-expressing or D2-expressing MSNs (at exactly the same coordinates of bilateral electrode array implantation stated above). DIO-ChR2-YFP virus (1 μ l, one site, 10^{12} titer) was injected through a glass pipette using a syringe pump (Nanoject II, Warner Instruments) precisely controlled by 0.2 Hz of 10 ms duration electrical pulses, and each pulse triggered 4.6 nl solution injection which the whole injection takes totally ~18min. The pipette was left in position for 5–10 min after the injection and then slowly moved out. The electrode array was the same as used for DS recording assembled but with a guide cannula attached (Innovative Neurophysiology, Durham, NC) terminating 300 μ m above the electrode tips; and was implanted into the same site >30 min later after viral injection, allowing for simultaneous electrophysiological recording and light stimulation. Following the implantation, a plastic cap was used to cover the cannula and animals were put back to homecage for two weeks allowing both viral expression and surgery recovery, before further training and recording experiments started.

Neuronal recording during behavior

The animals with implanted electrodes (Supplementary Table 1) were allowed to recover for 2 to 3 weeks after surgery before training started. The training procedure was exactly the same as described above for the animals only undergoing behavioral testing. Some animals took longer to acquire the task due to the mechanics of the recording wires, especially during the rapid sequence training stages (in total 3–5 weeks to reach FR4/0.5s, and some end up at FR4/1s). A subgroup of animals were also trained and recorded for two single-lever sessions each day with one session for left lever and another for right lever, to assess action-specific sequence activity. Another subgroup of animals were trained and recorded for two single-left-lever sessions each day with two consecutive schedules, to assess speed-specific sequence activity. For D1-/D2-MSNs identification during rapid sequence execution experiments, D1-Cre or D2-Cre mice were pretrained behaviorally before viral infection of ChR2 in order to match the timing of peak of ChR2 expression, surgery recovery and rapid sequence behavior.

Neural activity was recorded using the MAP system (Plexon Inc., TX). The spike activity was initially sorted using an online sorting algorithm (Plexon Inc.), and only cells with a clearly identified waveform and relatively high signal-to-noise ratio were used. In the end of recording, cells were resorted using an offline sorting algorithm (OfflineSorter, Plexon Inc.) to isolate single units. Single units displayed a clear refractory period in the inter-spike interval histogram, with no spikes during the refractory period (larger than 1.3 ms). TTL pulses were sent from a Med-Associates interface board to the MAP recording system through an A/D board (Texas Instrument Inc., TX) so that all animal's behavioral timestamps during sequence learning were synchronized and recorded together with the neural activity^{9,43}. For the simultaneous neuronal recording and optogenetic stimulation in D1-ChR2 and D2-ChR2 mice, the experiments were performed in another rig with the same operant box using the Cerebus recording system (Blackrock Microsystems, UT). Rather than that, all the spike recording and sorting procedures, and the simultaneously recorded

behavioral stamps as well as the light stimulation timing and duration, were processed in the same manner.

Striatal neurons classification

In dorsal striatum, fast-spiking interneurons - putative parvalbumin-containing neurons were identified as having a waveform half-width of less than 100 μ s with baseline firing rate of more than 10 Hz, and tonically active interneurons - putative choline acetyltransferase-expressing neurons were identified as those with a waveform half-width more than 300 μ s. All other units were classified as putative GABAergic medium-spiny projection neurons (MSNs)^{9,43}. Based on these criteria, 91.6% of all recorded striatal units were classified as MSNs, 3.4% as fast-spiking interneurons - putative parvalbumin-containing neurons and 5.0% as tonically active interneurons - putative choline acetyltransferase-expressing neurons, respectively (Supplementary Fig. 4 and Supplementary Fig. 9). For SNr and GPe, because of the rather small percentage of interneurons as well as the unknown physiological properties of them⁴⁴⁻⁴⁷, we regarded all cells recorded as putative GABAergic projection neurons. No animals were excluded from analyses. Putative FSIs and TANs recorded from the same electrode were excluded.

ChR2-aided D1-/D2-MSNs identification

The striatum consists of two major subpopulations of MSNs, with one subtype expressing dopamine D1 receptors and another subtype expressing dopamine D2 receptors^{18,22,48}. The DIO constructs used to express ChR2-YFP do not permit expression in cells that do not express Cre recombinase^{9,22,28,29}. Optical stimulation in ChR2-expressed cells was able to directly evoke spiking activity with short-latency^{9,22,28,29}. In present study, we connected the headstage and electrical wires for neuronal recording and the optic fiber for light stimulation from the beginning of the rapid sequence training session, for better monitoring of the same cells stably during behavioral training and later optogenetic identification. At the end of each training session, we delivered blue light stimulation through the optic fiber from a 473-nm laser (Laserglow Technologies, Toronto) via a fiber-optic patch cord, and simultaneously recorded the neuronal responses, to interrogate the molecular identity of cells previously recorded during the behavioral performance. The stimulation train was either 25 pulses of 10 ms duration delivered at 5 Hz or 14 Hz, or 25 pulses of 1000 ms duration delivered at 0.5 Hz. Multiple stimulation trains were repeatedly used based on the condition of the animal and quality of cell activity to verify cell identity. We very carefully regulated the laser power to a relatively low level, but strong enough to evoke reliable spikes in a small population of neurons recorded from certain electrodes, since high laser powers usually induced an electrical signal much larger and very different from the spike waveforms previously recorded in the same electrode, presumably resulting from synchronized activation of a large population of cells surrounding the electrode. For cell identification in different sessions in the same animal, significant effort was made to optimize the position of optic fiber in order to identify those units recorded from different electrodes and that were not being able to be identified in the previous session. The final laser power used for reliable identification of D1-/D2-MSNs was between 1.0 and 1.5 mW measured at the tip of the optical fiber (slightly varying for different mice and different sessions). Only those units showing very short (≤ 6 ms) response latency to light stimulation

and exhibiting exactly the same spike waveforms ($R = 0.95$, Pearson's correlation coefficient) during sequence behavior and light response were considered as direct activation and Cre positive^{9,28}. The results and the conclusions were qualitatively the same if a longer response latency was considered (< 10 ms). Although the latency of ChR2-evoked responses in D1-/D2-MSNs has been reported as being as long as 40 ms or more²², stricter criteria were employed in present study to minimize the possibility of false positives (with the risk of increasing false negatives, and hence having to perform more recordings/animals to achieve the same number of neurons). The final statistics was based on percentage of different activity types in individual animal so only those sessions successfully identified >3 cre-positive neurons were included for statistical analysis to avoid bias resulted from limited sampling size.

Analysis of neuronal activity

As described previously⁹, neuronal activity referenced to lever press onset was averaged in 20 or 50 ms bin, shifted by 1 ms, and averaged across trials to construct peri-event histograms (PETH) around lever pressing. Distributions of the PETH from 5000 to 2000 ms before lever press were considered baseline activity. We then determined which 20-ms bins, slid in 1 ms steps during an epoch spanning from 1000 ms before and after the event, met the criteria for task-related activity. A significant increase in firing rate was defined if at least 20 consecutive overlapping bins had firing rate larger than a threshold of 99 % above baseline activity, and a significant decrease in firing rate was defined if at least 20 consecutive bins had a firing rate smaller than a threshold of 95 % below baseline activity^{9,49}. The onset of press-related firing rate modulation was defined as the beginning of the first of 20 consecutive significant bins. The modulation period was defined as the time window from the beginning of the first of 20 consecutive significant bins to the final of the consecutive significant bins^{9,49}. To determine whether a task-related neuron was sequence start/stop related or not, we generated five firing-rate distributions, each one based on the PETH of rate modulation period for a specific press within the sequence: namely the first, second, third, fourth and final press within a sequence (the final was not always the fourth). Sequence start/stop related neurons were defined as those where the mean peak (or trough) firing-rate modulation of the first press (start), final press (stop), or both was significantly different from the peak/trough of the within sequence presses. Sequence-related inhibited or sustained types of neurons were determined in the same way by looking for those neurons that showed significantly negative or positive firing rate modulation for all lever presses within the sequence. To assess if neurons with sustained activity throughout pressing showed peaks of activity related to each lever press of the sequence, the first press related PETH was temporally shifted for the peak firing to match the timing of first lever press (as changes in neuronal activity typically preceded the first lever press)⁹ and the correlation coefficient was then calculated between the shifted PETH and the lever press rate histogram (also aligned to first press in the sequence). A procedure for classification of different types of sequence-related neuronal activity was based on a decision tree for determining sequence-related start/stop, sustained and inhibited types of neuronal activity, as well as potential subtypes with overlapping response. Principle component analysis (PCA) of individual-lever-press related firing rate modulation vector for the 1st, 2nd, 3rd and 4th press was conducted for further isolation of different response types. A 3-D classification was then

plotted based on first principle component (PC1), second principle component (PC2) and average modulation of neuronal firing rate of each neuron (Supplementary Figure 5). For D1-/D2-MSNs identification experiments, the neuronal response latency to light stimulation was defined as the beginning of significant firing rate increase after light onset, based on the neuron's baseline firing rate and light stimulation related PETH. All data analyses were conducted in Matlab with custom-written programs (MathWorks, MA).

Statistics

All statistics were performed on the basis of values for each animal per session. One-way ANOVA and repeated measures ANOVA were used to investigate general main effects; and paired or unpaired t-test (within or between subjects) was used in all planned and post-hoc comparisons; otherwise statistics were specifically stated in text. Samples sizes were calculated based on $\alpha = 0.05$ and power > 0.7 . Normality was verified for all analyses of variance. Statistical analyses were conducted in Matlab using the statistics toolbox (MathWorks, MA) and GraphPad Prism 4 (GraphPad Software, CA). Results were presented as mean \pm S.E.M., and statistical significance was considered for $P < 0.05$.

Supplementary Material

Refer to Web version on PubMed Central for supplementary material.

ACKNOWLEDGEMENTS

We thank C. Gerfen for the D1-Cre and D2-Cre mice, Y. Li for the RGS9-Cre mice, K. Nakazawa for the NMDAR1-loxP mice, G. Luo and A. Vaz for genotyping, and G. Cui for comments on the manuscript. This research was supported by the NIAAA Division of Intramural Clinical and Biological Research, the Champalimaud Neuroscience Programme, a European Research Council Grant 243393 to R.M.C. and the Whitehall Foundation, US National Institutes of Health Grant NS083815 to X.J.

REFERENCES

1. Lashley, KS. The problem of serial order in behavior. In: Jeffress, LA., editor. *Cerebral Mechanisms in Behavior*. New York: John Wiley Press; 1951.
2. Miller GA. The Magical Number Seven, Plus or Minus Two: Some Limits on Our Capacity for Processing Information. *Psychological Review*. 1956;81–97. [PubMed: 13310704]
3. Gallistel, CR. *The organization of action: A new synthesis*. Hillsdale, N. J.: Lawrence Erlbaum Associates, Inc.; 1980.
4. Doupe AJ, Kuhl PK. Birdsong and human speech: common themes and mechanisms. *Annu Rev Neurosci*. 1999; 22:567–631. [PubMed: 10202549]
5. Sakai K, Kitaguchi K, Hikosaka O. Chunking during human visuomotor sequence learning. *Exp Brain Res*. 2003; 152:229–242. [PubMed: 12879170]
6. Hikosaka O, Miyashita K, Miyachi S, Sakai K, Lu X. Differential roles of the frontal cortex, basal ganglia, and cerebellum in visuomotor sequence learning. *Neurobiol Learn Mem*. 1998; 70:137–149. [PubMed: 9753593]
7. Graybiel AM. The basal ganglia and chunking of action repertoires. *Neurobiol Learn Mem*. 1998; 70:119–136. [PubMed: 9753592]
8. Doupe AJ, Perkel DJ, Reiner A, Stern EA. Birdbrains could teach basal ganglia research a new song. *Trends Neurosci*. 2005; 28:353–363. [PubMed: 15935486]
9. Jin X, Costa RM. Start/stop signals emerge in nigrostriatal circuits during sequence learning. *Nature*. 2010; 466:457–462. [PubMed: 20651684]

10. Miyachi S, Hikosaka O, Miyashita K, Karadi Z, Rand MK. Differential roles of monkey striatum in learning of sequential hand movement. *Exp Brain Res*. 1997; 115:1–5. [PubMed: 9224828]
11. Benecke R, Rothwell JC, Dick JP, Day BL, Marsden CD. Disturbance of sequential movements in patients with Parkinson's disease. *Brain*. 1987; 110:361–379. [PubMed: 3567527]
12. Phillips JG, Chiu E, Bradshaw JL, Ianssek R. Impaired movement sequencing in patients with Huntington's disease: a kinematic analysis. *Neuropsychologia*. 1995; 33:365–369. [PubMed: 7792003]
13. Boyd LA, et al. Motor sequence chunking is impaired by basal ganglia stroke. *Neurobiol Learn Mem*. 2009; 92:35–44. [PubMed: 19249378]
14. Jog MS, Kubota Y, Connolly CI, Hillegaart V, Graybiel AM. Building neural representations of habits. *Science*. 1999; 286:1745–1749. [PubMed: 10576743]
15. Wymbs NF, Bassett DS, Mucha PJ, Porter MA, Grafton ST. Differential recruitment of the sensorimotor putamen and frontoparietal cortex during motor chunking in humans. *Neuron*. 2012; 74:936–946. [PubMed: 22681696]
16. Pellegrino F, Coupé C, Marsico E. A cross-language perspective on speech information rate. *Language*. 2011; 87:539–558.
17. Gerfen CR, et al. D1 and D2 dopamine receptor-regulated gene expression of striatonigral and striatopallidal neurons. *Science*. 1990; 250:1429–1432. [PubMed: 2147780]
18. Gong S, et al. Targeting Cre recombinase to specific neuron populations with bacterial artificial chromosome constructs. *J Neurosci*. 2007; 27:9817–9823. [PubMed: 17855595]
19. Albin RL, Young AB, Penney JB. The functional anatomy of basal ganglia disorders. *Trends Neurosci*. 1989; 12:366–375. [PubMed: 2479133]
20. DeLong MR. Primate models of movement disorders of basal ganglia origin. *Trends Neurosci*. 1990; 13:281–285. [PubMed: 1695404]
21. Graybiel AM. The basal ganglia. *Curr Biol*. 2000; 10:R509–R511. [PubMed: 10899013]
22. Kravitz AV, et al. Regulation of parkinsonian motor behaviours by optogenetic control of basal ganglia circuitry. *Nature*. 2010; 466:622–626. [PubMed: 20613723]
23. Hikosaka O, Takikawa Y, Kawagoe R. Role of the basal ganglia in the control of purposive saccadic eye movements. *Physiol Rev*. 2000; 80:953–978. [PubMed: 10893428]
24. Mink JW. The Basal Ganglia and involuntary movements: impaired inhibition of competing motor patterns. *Arch Neurol*. 2003; 60:1365–1368. [PubMed: 14568805]
25. Hampton CM, Sakata JT, Brainard MS. An avian basal ganglia-forebrain circuit contributes differentially to syllable versus sequence variability of adult Bengalese finch song. *J Neurophysiol*. 2009; 101:3235–3245. [PubMed: 19357331]
26. Aldridge JW, Berridge KC. Coding of serial order by neostriatal neurons: a "natural action" approach to movement sequence. *J Neurosci*. 1998; 18:2777–2787. [PubMed: 9502834]
27. Watanabe M, Munoz DP. Probing basal ganglia functions by saccade eye movements. *Eur J Neurosci*. 2011; 33:2070–2090. [PubMed: 21645102]
28. Lima SQ, Hromadka T, Znamenskiy P, Zador AM. PINP: a new method of tagging neuronal populations for identification during in vivo electrophysiological recording. *PLoS One*. 2009; 4:e6099. [PubMed: 19584920]
29. Boyden ES, Zhang F, Bamberg E, Nagel G, Deisseroth K. Millisecond-timescale, genetically targeted optical control of neural activity. *Nat Neurosci*. 2005; 8:1263–1268. [PubMed: 16116447]
30. Fujii N, Graybiel AM. Representation of action sequence boundaries by macaque prefrontal cortical neurons. *Science*. 2003; 301:1246–1249. [PubMed: 12947203]
31. Barnes TD, Kubota Y, Hu D, Jin DZ, Graybiel AM. Activity of striatal neurons reflects dynamic encoding and recoding of procedural memories. *Nature*. 2005; 437:1158–1161. [PubMed: 16237445]
32. Kimura M, Kato M, Shimazaki H, Watanabe K, Matsumoto N. Neural information transferred from the putamen to the globus pallidus during learned movement in the monkey. *J Neurophysiol*. 1996; 76:3771–3786. [PubMed: 8985875]
33. Tanji J. Sequential organization of multiple movements: involvement of cortical motor areas. *Annu Rev Neurosci*. 2001; 24:631–651. [PubMed: 11520914]

34. Hikosaka O. GABAergic output of the basal ganglia. *Prog Brain Res.* 2007; 160:209–226. [PubMed: 17499116]
35. McHaffie JG, Stanford TR, Stein BE, Coizet V, Redgrave P. Subcortical loops through the basal ganglia. *Trends Neurosci.* 2005; 28:401–407. [PubMed: 15982753]
36. Harvey CD, Coen P, Tank DW. Choice-specific sequences in parietal cortex during a virtual-navigation decision task. *Nature.* 2012; 484:62–68. [PubMed: 22419153]
37. Shima K, Tanji J. Binary-coded monitoring of a behavioral sequence by cells in the pre-supplementary motor area. *J Neurosci.* 2006; 26:2579–2582. [PubMed: 16510736]
38. Kao MH, Doupe AJ, Brainard MS. Contributions of an avian basal ganglia-forebrain circuit to real-time modulation of song. *Nature.* 2005; 433:638–643. [PubMed: 15703748]
39. Olveczky BP, Andalman AS, Fee MS. Vocal experimentation in the juvenile songbird requires a basal ganglia circuit. *PLoS Biol.* 2005; 3:e153. [PubMed: 15826219]
40. Graybiel AM, Rauch SL. Toward a neurobiology of obsessive-compulsive disorder. *Neuron.* 2000; 28:343–347. [PubMed: 11144344]
41. Vargha-Khadem F, Gadian DG, Copp A, Mishkin M. FOXP2 and the neuroanatomy of speech and language. *Nat Rev Neurosci.* 2005; 6:131–138. [PubMed: 15685218]

References

42. Dang MT, et al. Disrupted motor learning and long-term synaptic plasticity in mice lacking NMDAR1 in the striatum. *Proc Natl Acad Sci U S A.* 2006; 103:15254–15259. [PubMed: 17015831]
43. Burkhardt JM, Jin X, Costa RM. Dissociable effects of dopamine on neuronal firing rate and synchrony in the dorsal striatum. *Frontiers in Integrative Neuroscience.* 2009; 3:28. [PubMed: 19949467]
44. Gulley RL, Wood RL. The fine structure of the neurons in the rat substantia nigra. *Tissue Cell.* 1971; 3:675–690. [PubMed: 18631581]
45. Juraska JM, Wilson CJ, Groves PM. The substantia nigra of the rat: a Golgi study. *J Comp Neurol.* 1977; 172:585–600. [PubMed: 65369]
46. Millhouse OE. Pallidal neurons in the rat. *J Comp Neurol.* 1986; 254:209–227. [PubMed: 2432103]
47. Nambu A, Llinas R. Morphology of globus pallidus neurons: its correlation with electrophysiology in guinea pig brain slices. *J Comp Neurol.* 1997; 377:85–94. [PubMed: 8986874]
48. Gerfen CR. Indirect-pathway neurons lose their spines in Parkinson disease. *Nat Neurosci.* 2006; 9:157–158. [PubMed: 16439979]
49. Belova MA, Paton JJ, Morrison SE, Salzman CD. Expectation modulates neural responses to pleasant and aversive stimuli in primate amygdala. *Neuron.* 2007; 55:970–984. [PubMed: 17880899]
50. Paxinos, G.; Franklin, KB. *The mouse brain in stereotaxic coordinates.* 2nd edn. Academic Press; 2001.

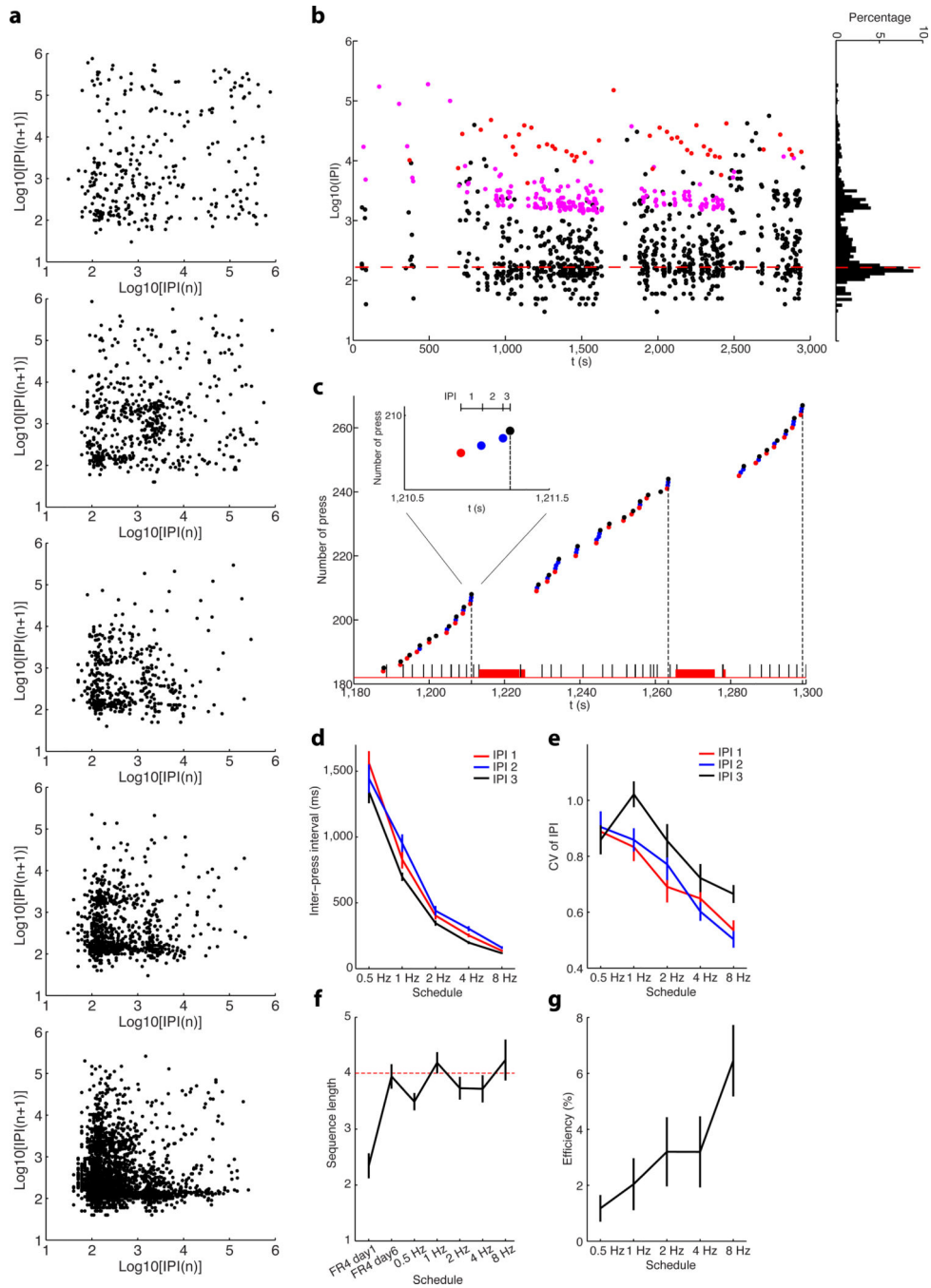


Figure 1. Behavioral learning of rapid action sequences in mice

a, Return map of inter-press intervals (IPIs) showing the behavior of same mouse across the different schedules. Every two consecutive IPIs contribute to one dot in the map. **b**, An example of single-session inter-press interval (IPI) dynamics of the same mouse as in **(a)** under schedule of FR4/0.5s. Each dot indicates an IPI. The short (black dots), intermediate (pink dots) and long (red dots) IPIs represent two lever presses performed in a chunk, two lever presses spaced by magazine checking without reward (i.e. headentry, no licks followed), and two lever presses spaced by reward consumption (i.e. licks), respectively.

Note that the first peak of the IPI distribution falls below 167ms (red dashed line) under the FR4/0.5s schedule. **c**, Behavioral microstructure of the same mouse performing under the FR4/0.5s schedule. Each dot indicates a lever press, with the red and black dots representing the first and final press within a sequence, and the blue dots intermediate presses. The vertical black dash lines imply the timing of reward. Black and red bars at the bottom indicate the timing of headentries and licks, respectively. Inset shows a rewarded lever press sequence. **d**, First, second and third IPI within a sequence changes across different schedules. **e**, Coefficient of variance for the first, second and third IPI across different training schedules. **f**, Sequence length during training under different schedules. **g**, Percentage of ultrafast sequences (FR4/0.5s) throughout training. Error bars denote SEM, same for all figures below.

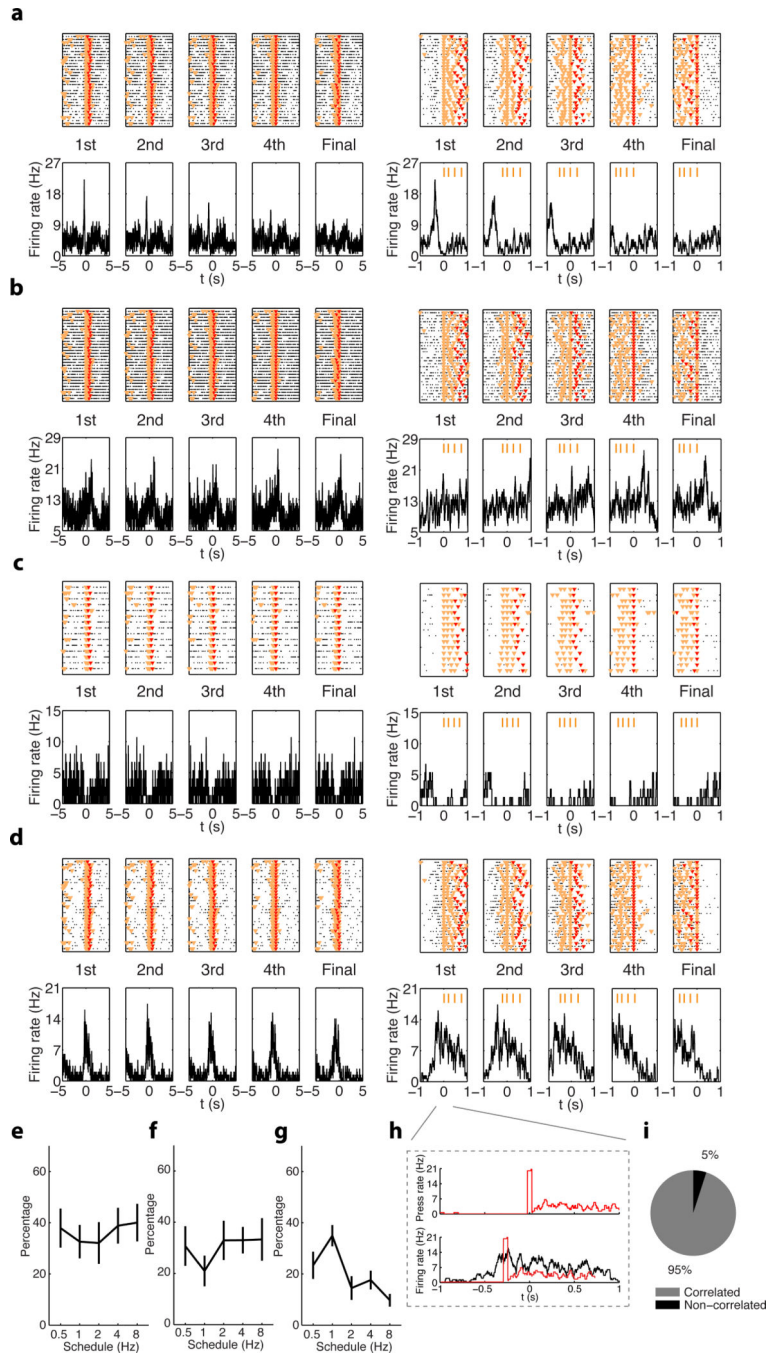


Figure 2. Neuronal activity in the dorsal striatum during learning and performance of rapid action sequences

a, Peri-event histogram (PETH) of a MSN related to each lever press within each rewarded action sequence under FR4/1s schedule. Top panels: each black dot indicates a spike and the orange and red triangle markers indicate lever pressing and reward timing, respectively (same markers used for all PETHs unless otherwise stated). Bottom panels: Average firing activity of the cell in relation to lever pressing, time zero indicates the time of lever pressing. Left and right five panels are PETHs from the same cell; the right PETHs were zoomed in to

show the fine temporal profile of the cell's activity, and the four orange bars on top mark the average timing for each press within sequence, same for all PETHs. This MSN shows phasic increase in firing activity selectively before the first lever press of each action sequence. **b**, PETH of a MSN showing phasic firing rate increase selectively after the final lever press of each action sequence. **c**, MSN showing a decrease in firing rate throughout the whole action sequence. **d**, MSN showing sustained firing activity throughout the whole action sequence. **e–g**, Statistic results of percentage of MSNs showing start/stop (**e**), inhibited (**f**) or sustained (**g**) sequence-related activity in the striatum across different schedules. **h**, Lever press histogram (top panel) and PETH for an MSN showing sustained activity (bottom panel), both referenced to the 1st lever press. The lever press histogram (bottom panel, red line) was temporally shifted to calculate the correlation with PETH (see Methods). **i**, Percentage of sequence-related MSNs with sustained activity that showed significant correlation between the PETH and the average lever press rate.

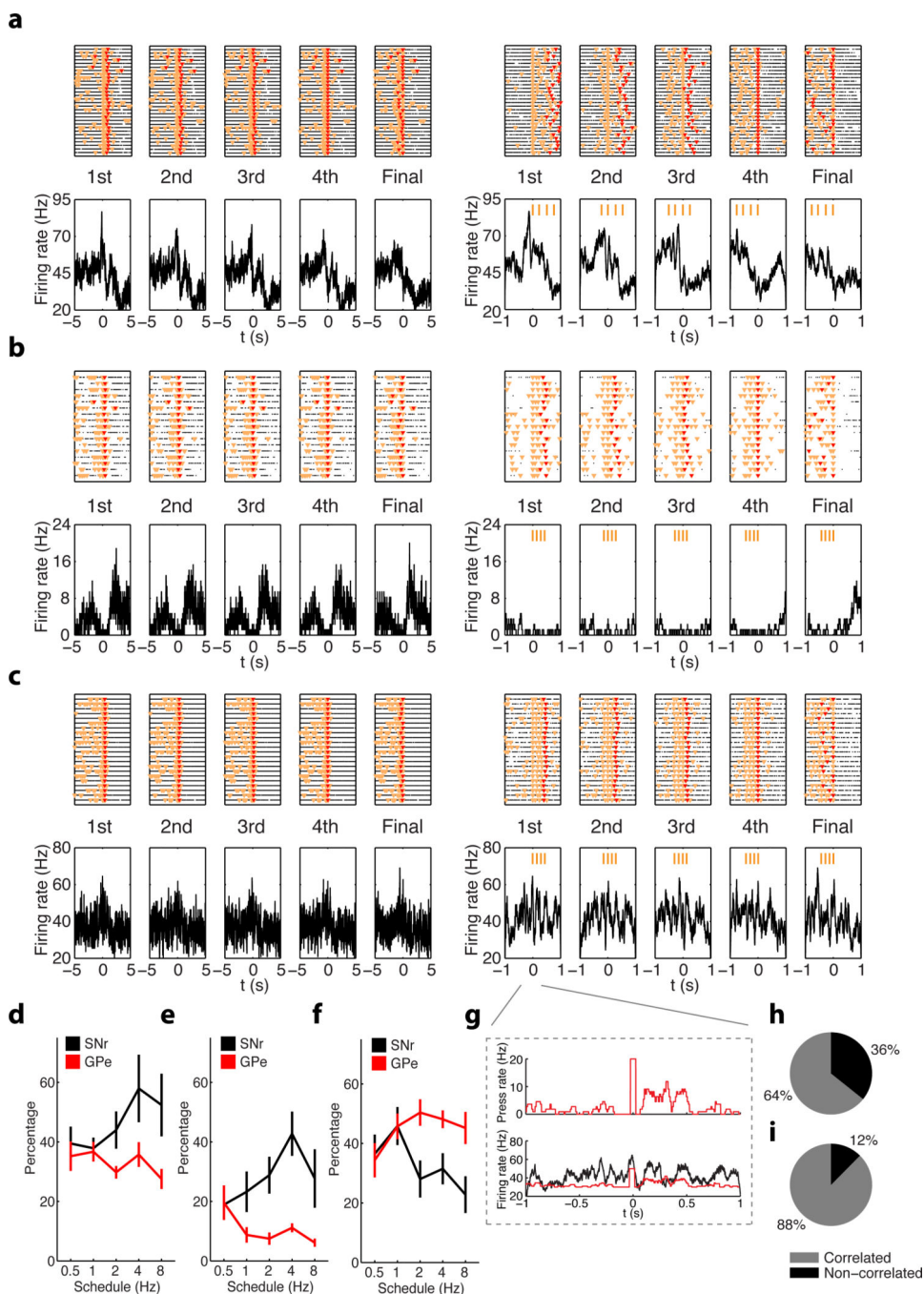


Figure 3. Neuronal activity in the SNr and GPe during learning and performance of rapid action sequences

a, A SNr neuron shows phasic firing rate increase selectively before the first lever press of each action sequence. **b**, A SNr neuron shows inhibited firing activity throughout the whole action sequence. **c**, A GPe neuron displays sustained firing activity throughout the whole action sequence. **d–f**, Percentage of SNr (black) and GPe (red) neurons showing start/stop (**d**), inhibited (**e**) or sustained (**f**) sequence-related activity during the performance of action sequences under different schedules. **h**, The lever press histogram (top panel) and the

sustained GPe neuron PETH (bottom panel) both aligned to the first lever press within action sequences. **i, j**, Percentage of neurons in SNr (**i**) and GPe (**j**) displaying sequence-related sustained activity with significant correlation between PETH and average lever press rate.

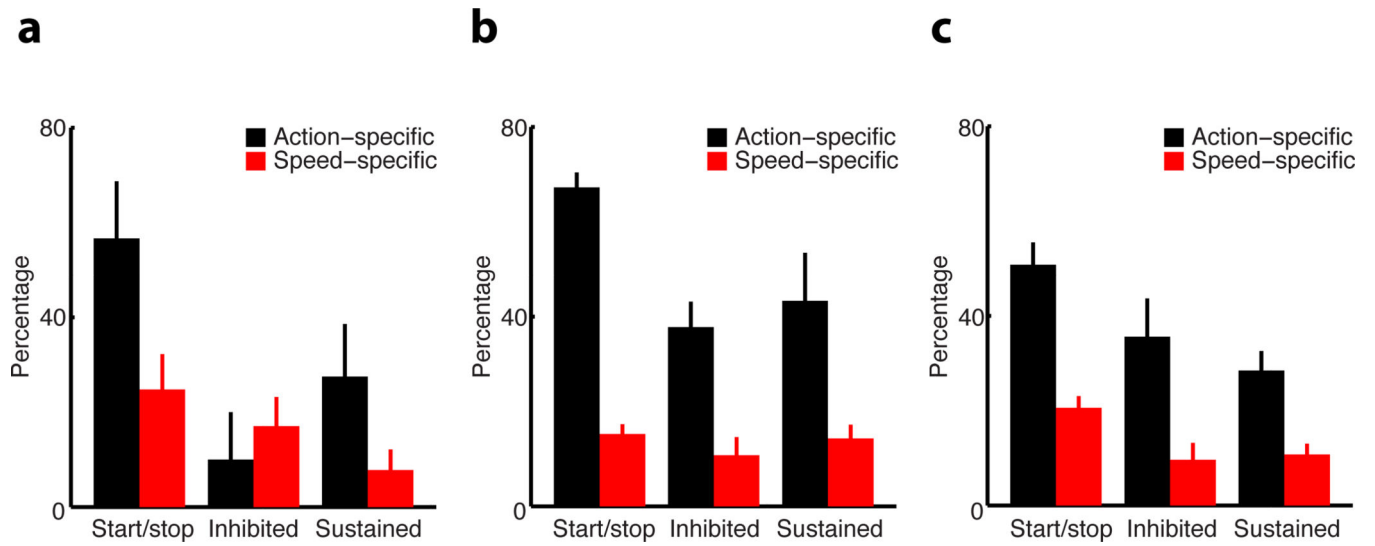


Figure 4. Action- vs. speed-specific sequence-related activity in the basal ganglia circuits
a–c, Percentage of action-specific (black bars) and speed-specific (red bars) start/stop, inhibited and sustained activity in striatum (**a**), SNr (**b**) and GPe (**c**), respectively.

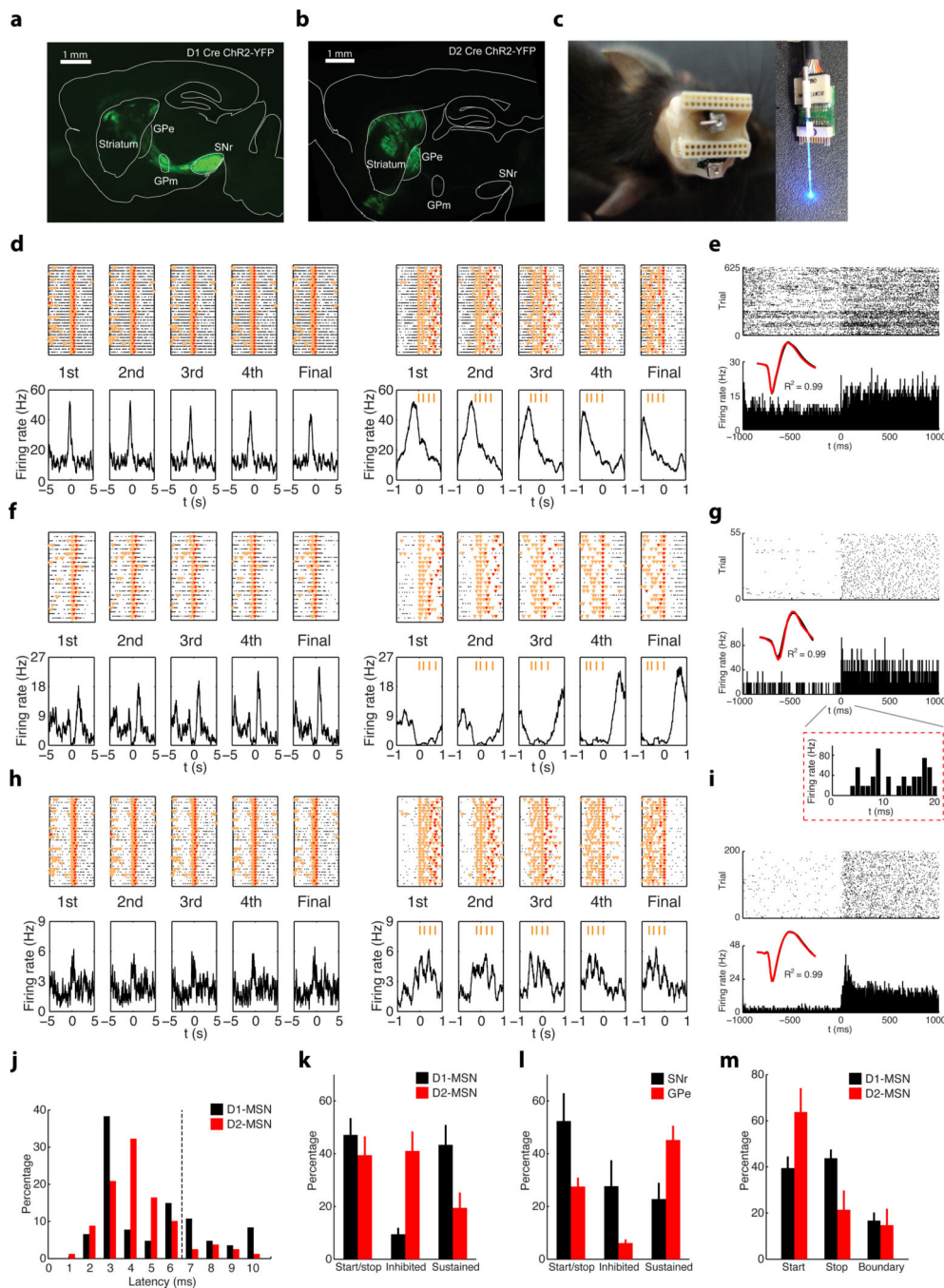


Figure 5. Subcircuit-specific neuronal activity in the basal ganglia during learning and performance of rapid action sequences

a, A coronal section of dorsal striatum from a D1 Cre mouse with viral driven expression of ChR2-YFP; note axons targeting GPM and SNr. Scale bar 1mm. **b**, A coronal section of dorsal striatum from a D2 Cre mouse with viral driven expression of ChR2-YFP; note axons targeting GPe. Scale bar 1mm. **c**, Illustration of electrode array and cannula design allowing for adjustable fiber optic stimulation for cell identification. **d**, PETH of a MSN recorded in a D1-ChR2 mouse, showing sequence start related activity. **e**, Same neuron as (**d**) evident by

identical waveform (black trace during action sequences vs. red trace during light stimulations, same for below) showed reliable, short-latency response to blue light stimulation. **f**, PETH of a MSN recorded in a D2-ChR2 mouse, showing sequence-related inhibited activity. **g**, Same neuron as (**f**) shows reliable, short-latency response to blue light stimulation at the end of session. Inset panel showing the neuronal response to light stimulation at fine time scale. **h, i**, PETH of a MSN recorded in a D1-ChR2 mouse, showing sequence-related sustained activity (**h**), and its response to light stimulation at the end of the session (**i**). **j**, Distribution of light to response latencies for D1- and D2-MSNs. **k, l**, Proportions of striatal D1- and D2-MSNs (**k**), and SNr and GPe neurons (**l**) displaying different types of sequence-related activity under FR4/0.5s. **m**, Percentage of striatal D1- or D2-MSNs displaying sequence start, stop, or boundary-related activity.